Thermally Induced Solid-State Phase Transition of Bis(triisopropylsilylethynyl) Pentacene Crystals

Jihua Chen,[†] John Anthony,[||] and David C. Martin*[,†,‡,§]

Macromolecular Science and Engineering, Materials Science and Engineering, Biomedical Engineering, The University of Michigan, 2300 Hayward Street, Ann Arbor, Michigan 48109, and Department of Chemistry, The University of Kentucky, Lexington, Kentucky 40506

Received: May 7, 2006; In Final Form: June 23, 2006

Bis(triisopropylsilylethynyl) pentacene (TIPS pentacene) is a functionalized pentacene derivative designed to enhance both the solution solubility and solid-state packing of pentacene. In this paper, we report our observations of a solid-state phase transition in TIPS pentacene crystals upon heating or cooling. Evidence from differential scanning calorimetry (DSC), hot-stage optical microscopy, as well as high-temperature X-ray and electron diffraction are presented. A reasonable match with experimental data is obtained with molecular modeling. Our results reveal that the transition is associated with a conformational reorganization of the TIPS side groups, accompanied by a slight decrease in the acene-to-acene spacing and a shift of the overlap between the neighboring pentacene units. The observed cracking should be avoided or minimized in TIPS pentacene-based thin film transistors to maintain their relatively high charge carrier mobility.

Introduction

With their enormous variability and potentially low-cost fabrication, organic electronic materials have attracted significant recent commercial and scientific interest. In particular, pentacene has been extensively studied as an organic molecular semiconductor in various thin film applications.[1−3] However, pentacene is not soluble in any convenient organic solvents, which rules out its use in solution processing. In addition, pentacene molecules are known to adopt a herringbone structure in the crystal, so that their lateral $\pi-\pi$ overlap interactions are not optimized. Although pentacene, with its measured mobility values as high as 1.5 $cm^2/V\cdot s$,[4] is currently among the organic materials with highest charge carrier mobilities known, it is believed that there still could be improvements in pentacene's mobility if its $\pi-\pi$ interactions could be enhanced.

Bis(triisopropylsilylethynyl) pentacene (TIPS pentacene) was synthesized to address precisely these limitations (Figure 1). On one hand, the TIPS side groups make TIPS pentacene soluble in common organic solvents; on the other hand, these bulky groups also help to disrupt the face-to-edge herringbone packing pattern and to form a regular columnar stacking between acene planes.[5,6] The effects of temperature, pressure, and iodine doping, as well as the crystallographic anisotropy on the electrical resistivity of TIPS pentacene single crystals have been examined previously.[7] In addition, extended Huckel theory (EHT) calculations of band electronic structure,[8] thin film transistor characteristics,[9] and photoconductivity[10] have been reported for this organic semiconductor and have been compared to either unmodified pentacene or pentacene derivatives with other side groups (such as trimethylsilylethynyl TMS). Recent ultrafast photoconductivity experiments suggest that, in TIPS pentacene thin films, there is band-like charge carrier transport at subpicosecond time scales.[11]

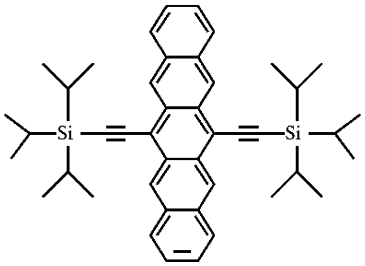

Figure 1. Molecular structure of TIPS pentacene.

The thermal properties of organic molecular semiconductors could be critical for thin film applications, not only because the elevated substrate temperature sometimes adopted in fabrication may form crystalline grains with larger domain sizes but also because of the end-use requirements in different applications. In this paper, we report on a thermally induced solid-state phase transition in crystalline TIPS pentacene thin films. This phase transition leads to the formation of crystallographically well-defined cracks throughout the TIPS pentacene crystals. This phase transition should be avoided or at least minimized in fabrication and application of TIPS pentacene-based thin film transistors to maintain their relatively high charge carrier mobility.

Experiments

Materials. The synthesis of TIPS pentacene is published elsewhere.[6] The TIPS pentacene crystals are dark blue and adopt needle or platelet shapes. According to single-crystal X-ray diffraction results, perfect, long, needle-shaped TIPS pentacene crystals have the long axis parallel to the [100] direction.

Thin Film Formation. TIPS pentacene thin films were prepared from solution casting using a 0.1 wt % toluene solution. Samples for hot-stage optical microscopy were allowed to slowly crystallize from solution in a covered glass Petri dish, while

* To whom correspondence should be addressed. E-mail: milty@umich.edu.
[†] Macromolecular Science and Engineering, The University of Michigan.
[‡] Materials Science and Engineering, The University of Michigan.
[§] Biomedical Engineering, The University of Michigan.
[||] Department of Chemistry, The University of Kentucky.

10.1021/jp0627877 CCC: $33.50
Published on Web 08/03/2006

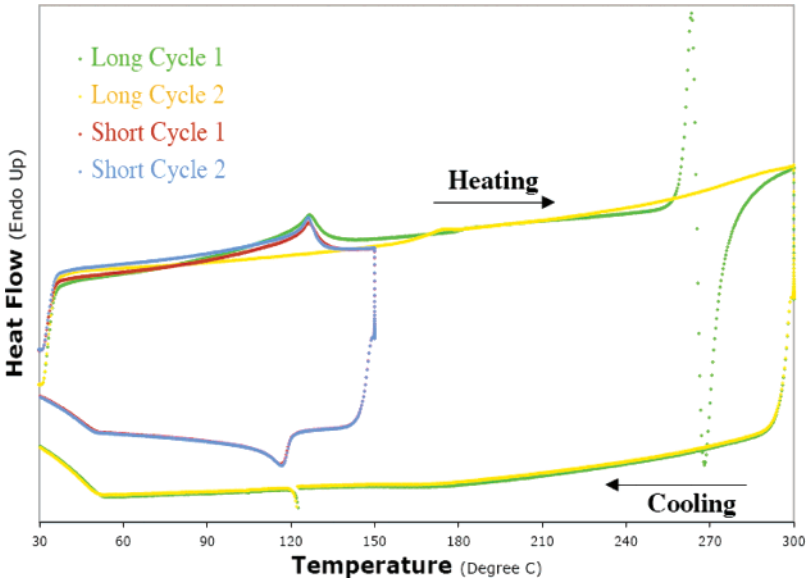

Figure 2. Differential scanning calorimetry of TIPS pentacene (heating and cooling rates were 10 °C/min, and scans were done in nitrogen). (1) Long Cycles 1 and 2 were done on the same sample sequentially. A characteristic endothermic transition at 124−127 °C was observed in Long Cycle 1, followed by endothermic melting and exothermic degradation at 261 and 266 °C, respectively. The absence of all these three peaks in Long Cycle 2 indicates a complete degradation of TIPS pentacene. (2) Short Cycles 1 and 2 were also done on the same sample in sequence. The characteristic 124 °C transition is mostly reversible, suggesting a solid-to-solid-phase transition.

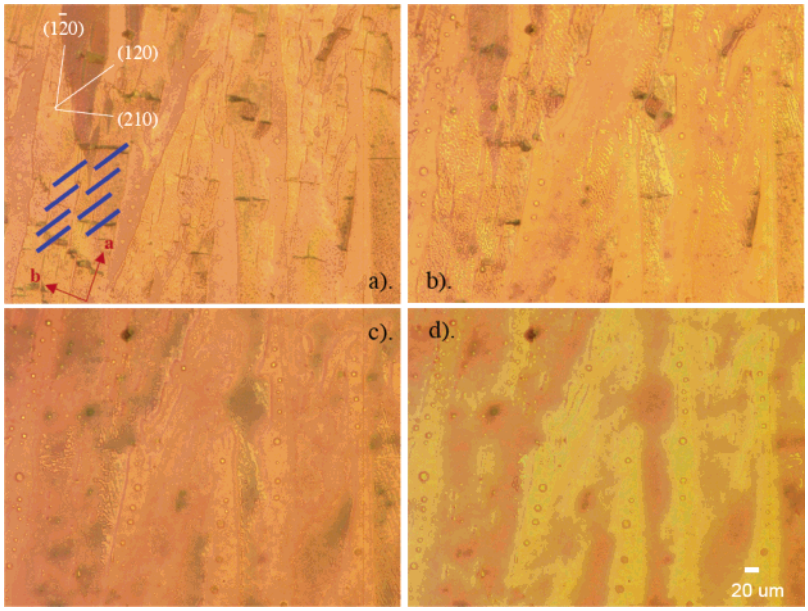

Figure 3. Hot-stage optical micrographs of TIPS pentacene corresponding to the melting and degradation in the Long Cycle 1 of the DSC results in Figure 2. Pictures were taken in ambient condition as a time series, with image (d) being the last one. The same sample was heated again as in Long Cycle 2 of the DSC experiment (Figure 2); however, the thin film morphology did not change much from image (d) through the whole process. Notice that samples in image (a) maintained their birefringence quite well, whereas samples in image (d) did not.

samples for hot-stage TEM experiments were dried in air to achieve thinner films. Hot-stage optical microscopy samples were deposited on a clean glass cover slip. TEM samples used a thin layer of amorphous carbon (∼50 nm) deposited on regular 3-mm copper grids (400 mesh, from Ted Pella).[12]

Differential Scanning Calorimetry (DSC). A Perkin-Elmer DSC6 and Pyris Thermal Analysis System 3.52 were utilized in the DSC experiments. Samples were ground into fine powders to minimize the influence of crystal size and shape, and sample weights were always kept between 5 and 10 mg. Heating and cooling rates were all 10 °C/min. At the lowest and highest temperatures in the thermal cycles, the samples were held isothermally for 1 and 5 min, respectively. Nitrogen gas was consistently flushing the system during all experiments.

Hot-Stage Optical Microscopy. A Linkam TH 1500 hot stage with a TMS 91 controller, a Spot RT Color 2.2.1 CCD camera (from Diagnostic Instruments, Inc.), and a Nikon OptiPhot2-POL optical microscope were combined in one system to monitor the structural changes during thermal cycling of the TIPS pentacene thin films. Heating and cooling rates were set to be 10 °C/min and holding times at the highest temperatures were 5 min, as in the DSC experiments.

Hot-Stage X-ray Diffraction. TIPS pentacene samples were ground into powders and then examined during temperature scans with a Bruker-AXS D8 Advance powder X-ray diffraction system. Samples were held at each scanning temperature for about 24 min (scanning rate, 2°/min; two theta angle scanning

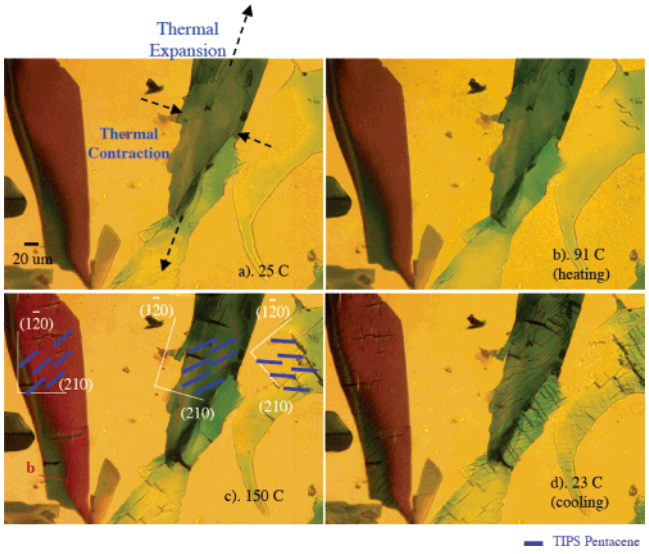

Figure 4. Hot-stage optical micrographs of TIPS pentacene corresponding to Short Cycle 1 of the DSC results in Figure 2.

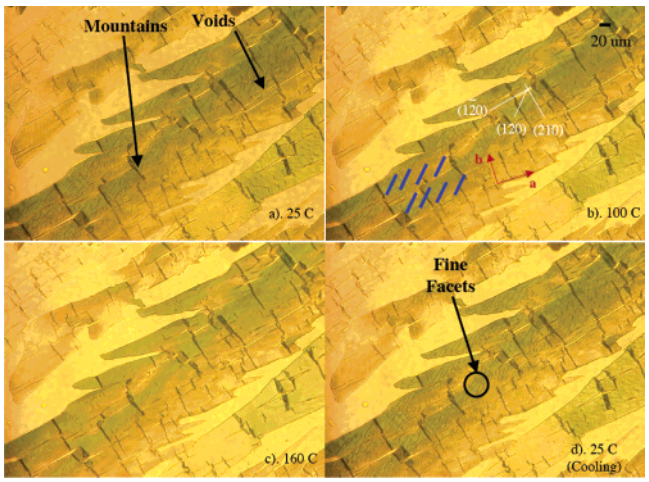

Figure 5. Hot-stage optical micrographs of TIPS pentacene corresponding to Short Cycle 2 of the DSC results in Figure 2.

range, 3−50°). Heating and cooling rates between the temperature scans were 6 °C/min.

Hot-Stage TEM and Selected Area Electron Diffraction (SAED). TEM experiments were conducted at 120 kV on a Philips CM12 with a Gatan 628-0500 Thermal Stage. Heating and cooling rates were about 10 °C/min, and samples were held at 133 °C (well above the 124 °C thermal transition temperature) for more than 5 min before taking data.

Molecular Simulations. Cerius[2] modeling software from Accelrys was employed to simulate various diffraction results and provide visualizations of models. The room-temperature model was obtained from single-crystal X-ray diffraction analysis. Unit cell parameters of the high-temperature model were estimated from hot-stage XRD and hot-stage SAED experiments well above the 124 °C thermal transition point. Since the Compass force field was found to minimize the energy of the room-temperature model without much variation from the experimentally determined unit cell parameters, the high-temperature unit cell parameters were applied to the room-temperature model and the molecule was allowed to minimize its total energy with the Compass force field, keeping the unit cell dimensions constrained.

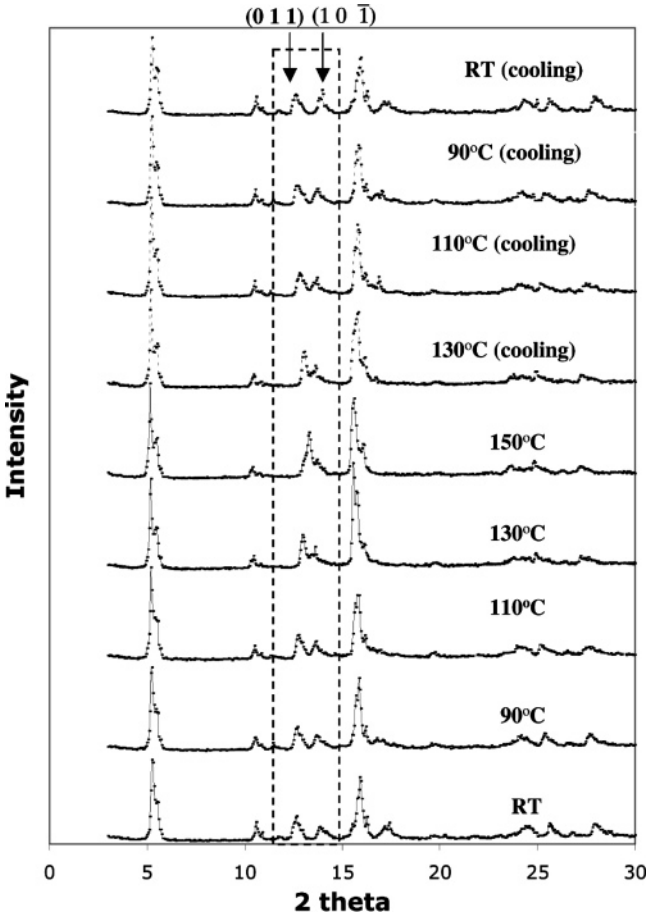

Figure 6. Hot-stage XRD of TIPS pentacene corresponding to Short Cycle 1 of the DSC results in Figure 2.

Results and Discussion

DSC. In Figure 2, the long thermal cycles were scanned from 30 to 300 °C, while the short ones were from 30 to 150 °C only. Notice that Long Cycle 2 was done on the same sample as Long Cycle 1 but after the sample went through Long Cycle 1. A characteristic endothermic peak at 124 °C was observed in Long Cycle 1, followed by an endothermic melting at 261 °C with exothermic degradation shortly thereafter at 266 °C. The absence of all these three peaks in Long Cycle 2 indicated complete decomposition of TIPS pentacene, most likely by Diels−Alder polymerization between the alkyne substituent and the pentacene backbone.

Short Cycles 1 and 2 were also done sequentially. The characteristic 124 °C transition was largely reversible, suggesting a solid-state phase transition, as this temperature was far below the melting point (261 °C). This endothermic peak in the heating cycles, with an enthalpy change of 25.6 J/g, also turned out to be a rather broad transition that started around 90 °C and ended at about 133 °C. In addition, during cooling, the structure was able to consistently transform backward at 116 °C.

Hot-Stage Optical Microscopy. Different thermal cycles corresponding to the four DSC curves in Figure 2 were used in hot-stage optical microscopy. The morphology changes during melting and subsequent degradation in Long Cycle 1 are shown in Figure 3. Faceted crystalline films gradually turned into small brown amorphous droplets during isothermal annealing at 250 °C (in air). This melting temperature was slightly lower than the one detected by DSC (261 °C), most likely because DSC was done with samples in a nitrogen atmosphere, whereas optical microscopy experiments were conducted under ambient

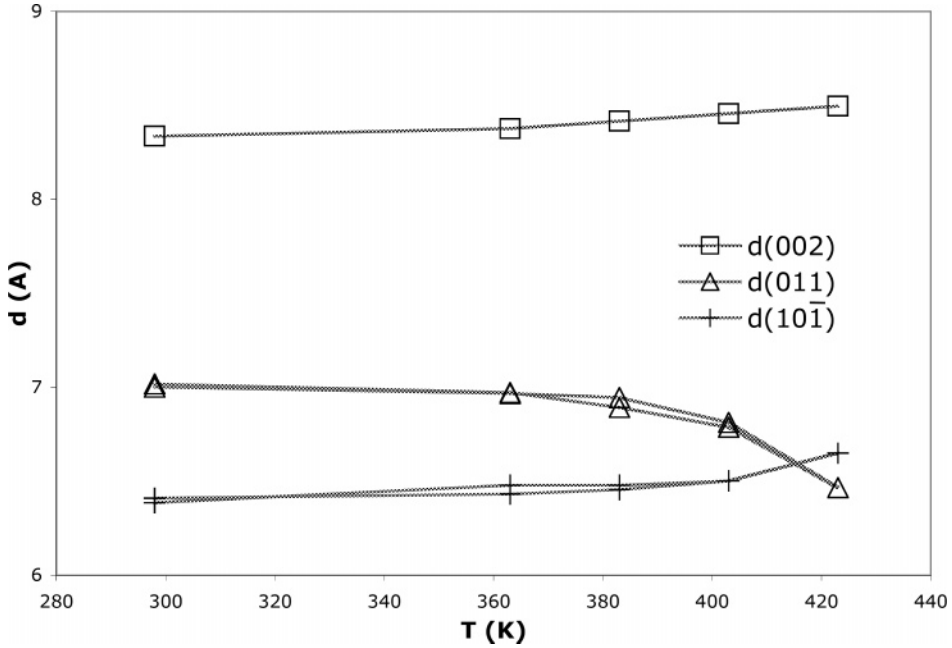

Figure 7. Interplanar *d* spacing changes of TIPS pentacene upon heating and cooling, measured from hot-stage XRD data, during Short Cycle 1 of the DSC results in Figure 2.

conditions. In addition, polarized light microscopy showed that the initial films (Figure 3a) were highly birefringent; whereas after heating the films were almost totally isotropic (Figure 3d). The amorphous films formed in Long Cycle 1 did not change further in any significant way during Long Cycle 2, which agrees with the DSC results since the structural change due to degradation was not reversible during cooling.

On the other hand, the transition at 124 °C did have some reversible features seen in the optical microscope. Figures 4 and 5 were taken during thermal scans corresponding to Short Cycles 1 and 2 in Figure 2. The edges along the long axis of the TIPS pentacene films were determined as (1$\bar{2}$0) according to electron diffraction experiments. Although the crystallographic cracking in Short Cycle 1 also remained in Short Cycle 2, many additional fine facets that were predominantly along (120) in Short Cycle 2 were identified, which appeared only at lower temperatures.

With more careful examination, the cracking was found to be associated with characteristic changes in the dimensions of the crystals. Upon heating, the TIPS pentacene thin films tend to expand along the long axis. At the same time, they contract perpendicular to their long axis. Therefore, the crystals form voids that are always oriented parallel to the long axis of the film, whereas there is crystal overlapping perpendicular to the long axis. The voids along the long axis were parallel to the plane (1$\bar{2}$0), while the "mountains" caused by overlapping were parallel to (210). The crystal in the middle of parts a−d of Figure 4 was estimated to contract along its short axis by 6.9% and expand along its long axis by 5.6%; the crystal on the left (Figure 4) contracted and expanded by 5.3% and 2.9%, respectively. These strains are expected to be highly sensitive to substrate interactions and local molecular confinement. With more expansion and contraction measurements (10 in total), an average expansion value of 3.9 ± 1.0% was obtained and the calculated contraction along short axis was 7.5 ± 1.7%.

Hot-Stage XRD, Hot-Stage TEM/SAED, and Molecular Simulation. By comparing results from optical microscopy with those obtained by bright field TEM, we found that the detailed morphology of the TIPS pentacene films was a function of the film thickness. The thinnest films (less than ∼50 nm) were discontinuous, with individual TIPS pentacene crystalline domains. Thicker films were more continuous and showed larger crystallites. The nature of the cracking was also found to change with film thickness. The thinnest films primarily showed cleavage on the (120) and (1$\bar{2}$0) planes, whereas those of the thicker films (more than ∼200 nm) also showed cracks propagating on the (210) planes. This change in cracking behavior with film thickness may be due to thermally induced strains associated with the shape change during the phase transition.

A thermal cycle corresponding to Short Cycle 1 of the DSC results was used for powder XRD experiments (Figure 6). The relationship between temperature and *d* spacing of different crystallographic planes was extracted for several planes including (002), (011),and (10$\bar{1}$) (Figure 7). The unit cell parameter *c* only increases slightly with temperature in the testing range, as suggested by the slight increase of (00$\bar{1}$) and (002) spacing. The substantial changes in (011) and (10$\bar{1}$), which correspond to the larger increase in *a* and decrease in *b* upon heating, more clearly represent the main features of this phase transition.

A pattern that frequently occurred in SAED experiments is shown in Figure 8, and this matched well with the expected [001] projection of the room-temperature model of the TIPS pentacene (the so-called "low-temperature model"). This indicated that the TIPS pentacene molecules were lying on the substrate with their acenes almost vertical to the substrate plane and the bulky side groups touching down (Figure 9). This strong in-plane crystallographic texturing of the TIPS pentacene film, with the (001) planes parallel to the substrate, was also confirmed with 2D X-ray diffraction patterns taken with a near-grazing incident angle.

With regard to both spacing and angle, the TIPS pentacene [001] SAED patterns above the 124 °C thermal transition were noticeably different from those at room temperature (Figure 10). The obvious increase in *a* and decrease in *b* beyond the transition point, demonstrated by the increased (100) but decreased (010) spacing, also agreed well with the results in hot-stage XRD. At the same time, this observation explained the characteristic cracking in hot-stage optical micrographs. Since the *a* direction is close to the long axis of the thin film (or [210] direction)

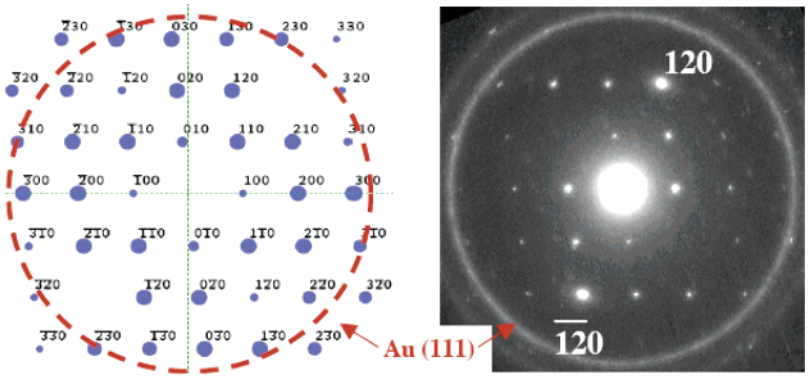

Figure 8. Selected area electron diffraction (SAED) of TIPS pentacene at room temperature. Left: [001] projection simulated with the low-temperature model by Cerius.[2] Right: A frequently observed experimental pattern. Rings are from gold calibration: 0.2355 nm for an Au(111) plane.

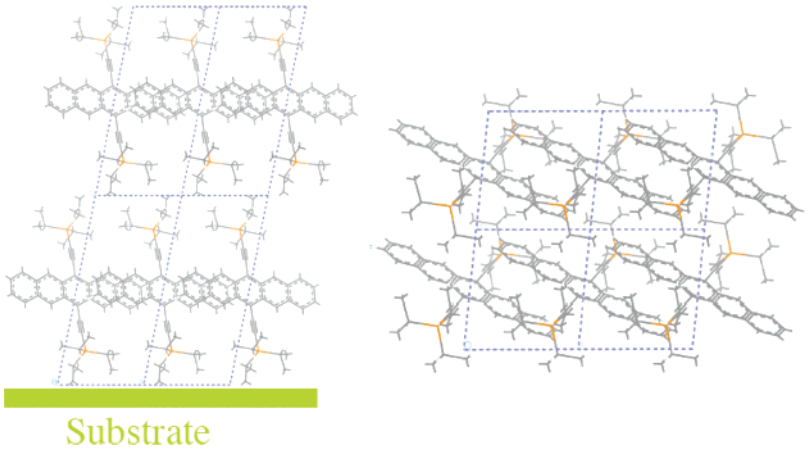

Figure 9. Often-occurring [001] patterns of TIPS pentacene suggest that TIPS pentacene has a side-group edge-on orientation in solution-processed thin films. Left: side view of TIPS pentacene on substrate ([010] zone). Right: top view of TIPS pentacene on substrate ([001] zone).

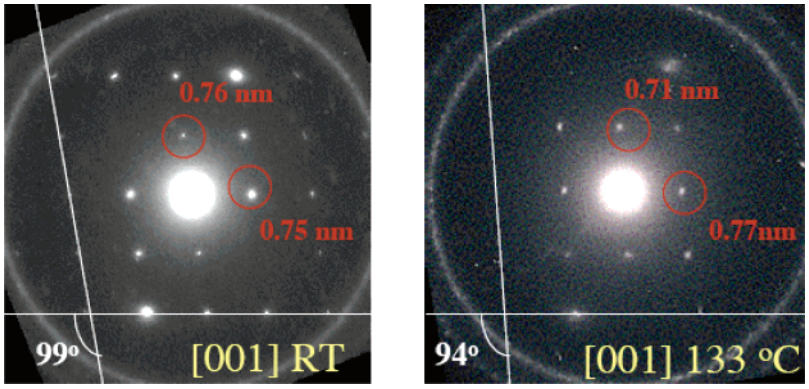

Figure 10. Comparison between experimental [001] SAED patterns of low-temperature and high-temperature TIPS pentacene crystals. There were both *d* spacing and angle changes.

and *b* is close to the short axis,[13] an increased value of *a* at high temperature can generate cracks that are apparently caused by overlapping and perpendicular to the long axis of the TIPS pentacene film, while a significantly reduced *b* value causes the cracks which are essentially voids and were predominantly parallel to the long axis of the thin films (Figure 4).

A set of unit cell parameters for high-temperature TIPS pentacene were estimated from the powder XRD results and electron diffraction data obtained well above the 124 °C transition point. Compared to the best-fit unit cell parameters for the low-temperature phase ($a = 0.755$ nm, $b = 0.773$ nm, $c = 1.676$ nm, $\alpha = 89.5$, $\beta = 78.7$, $\gamma = 84.0°$), the cell parameters of the high-temperature phase were $a = 0.780$ nm, $b = 0.720$ nm, $c = 1.720$ nm, $\alpha = 90.0$, $\beta = 85.0$, $\gamma = 88.0°$. This high-temperature unit cell model was then used in molecular simulations, and the calculated SAED [001] pattern and powder XRD at high temperature were compared with those of the low-temperature phase (Figures 11 and 12). These simulation results were a reasonable fit with the available experimental data as shown in Figures 10 and 6.

Comparing the two TIPS pentacene models at different temperatures, we obtained a characteristic expansion of 3.3% for cell parameter *a* and a contraction of 6.9% for *b*. Those values turned out to agree well with the crystal dimension changes measured from the optical images. The contraction along (210) or film short axis was 7.5 ± 1.7%, while an expansion of 3.9 ± 1.0% was measured for the $(1\bar{2}0)$ direction or film long axis. Since axis *a* of the TIPS pentacene unit cell

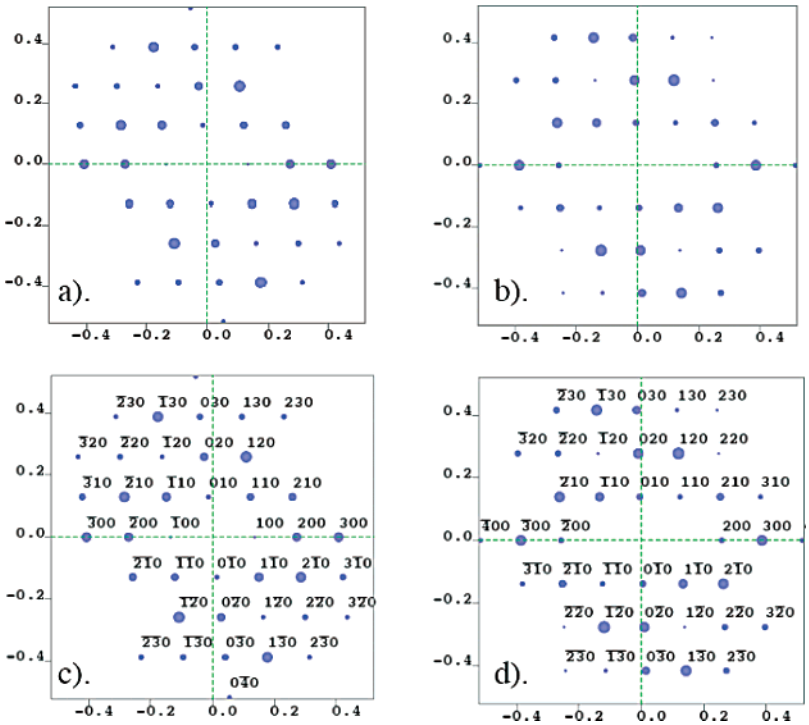

Figure 11. Simulated TIPS pentacene [001] patterns at low (a and c) and high temperature (b and d). Images a and b are the versions without indexing, and images c and d are the ones with indexing.

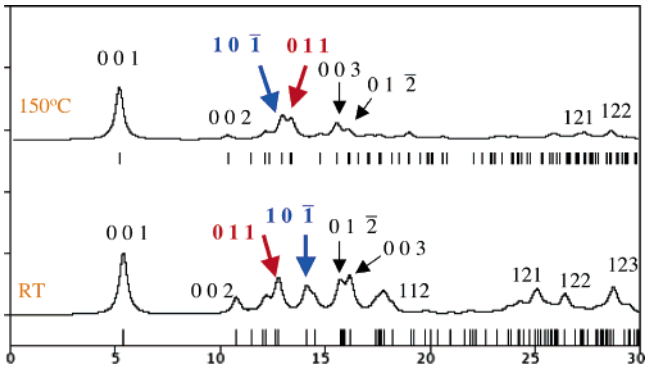

Figure 12. Simulations of hot-stage XRD of TIPS pentacene with the low- and high-temperature models.

is about 25° off the long axis of thin films at room temperature, and *b* is 25° off the short axis, the corresponding expansion of cell parameter *a* was estimated to be 3.9%*cos 25° = 3.5%, and the contraction of *b* was 7.5%*cos 25° = 6.8%.

Different views of the two TIPS pentacene crystal models were compared in various directions. Figure 13 shows projections of both models viewed along the [111] direction of the low-temperature cell. Obvious differences between the models include their side-group conformation and the extent of acene overlapping. In the high-temperature model, the total $\pi-\pi$ stacking area was slightly reduced from approximately 7.7 to 7.3 Å^2 per one TIPS pentacene molecule, if the acenes were simplified as rectangles in "pitched" or "rolled" π-stacks.[14] Figure 14 shows the images viewed down the acene plane of the low-temperature model. The rigid pentacene units become closer to each other by an estimated 0.22 Å.

The driving force for this phase transition is believed to be the onset of conformational freedom in the TIPS side groups as the temperature is raised, leading to a change in the geometry of the unit cell that causes the macroscopically observed crystallographically regular cracking. For TIPS pentacene, we expect that this cracking will make it more difficult for charge

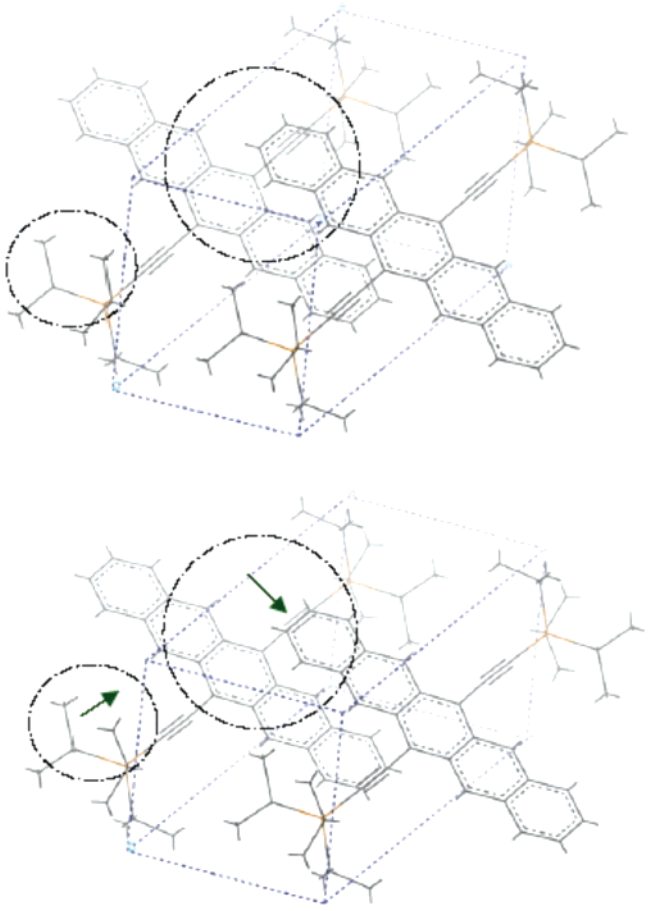

Figure 13. Low-temperature (top) and high-temperature TIPS pentacene models (bottom) viewed down the [111] zone of the low-temperature model.

to be transported through the crystal, leading to an inevitable decrease in the experimentally observed carrier mobility. Since

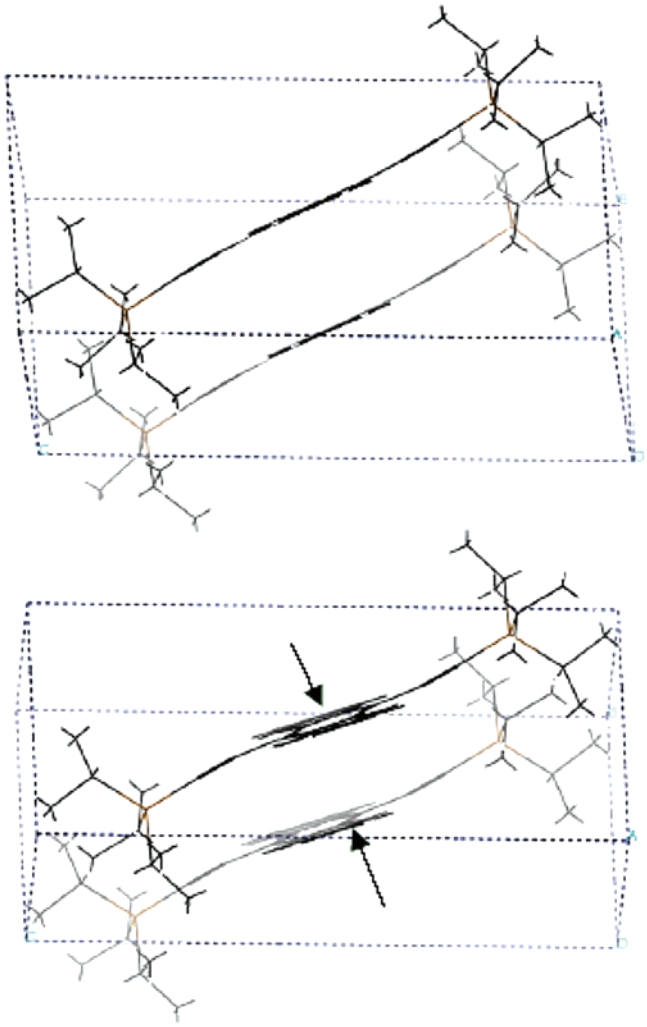

Figure 14. Low-temperature (top) and high-temperature TIPS pentacene models (bottom) viewed down the acene plane of the low-temperature model.

there is a decrease in the $\pi-\pi$ stacking distance in the high-temperature phase, there is the potential that a similar change in solid-state packing could be used to design a material with improved performance, particularly if the associated cracking could be minimized or avoided.

Conclusions

A structural phase transition near 124 °C was observed in TIPS pentacene crystals upon heating or cooling with DSC, hot-stage optical microscopy, variable temperature XRD, and SAED. Crystallographically regular cracking accompanied the transition. Thermal expansion along and contraction across the long axis of the single crystals in the TIPS pentacene film caused obvious overlapping along and voids across the film long axis. These microscopic observations agree well with the electron diffraction and X-ray diffraction results that, when heated from 30 to 150 °C, unit cell parameter *a* increases, while *b* decreases significantly. Cell parameters well beyond the transition point were estimated from diffraction experiments, and a reasonable fit between our experiments and molecular simulation was achieved. According to these models, during the phase transition from low to high temperature, the distance between acene planes becomes slightly closer, the overlapping area of acene units reduces, and at the same time there is a rearrangement of the bulky TIPS side groups.

Acknowledgment. The authors would like to thank the NSF for financial support (DMR-0084304 and DMR-6518079). The low-temperature model of TIPS pentacene was generated by single-crystal XRD with the assistance of Dr. Jeff Kampf. Variable temperature XRD data were collected in Prof. Omar M. Yaghi's lab in the Department of Chemistry at the University of Michigan at Ann Arbor. Jesse Rowsell, Hyunsik Moon, and John Nanos helped us with this experiment. Technical staff Ying Qi at the Materials Science and Engineering department made a lot of efforts in repairing and maintaining our optical microscopy hot stage, X-ray diffraction, and DSC equipment. TEM studies were conducted at the Electron Microbeam Analysis Laboratory at the University of Michigan at Ann Arbor, with kind assistance from the lab managers, Dr. Carl Henderson, Dr. John Mansfield, and Dr. Kai Sun. J.C. appreciates constructive discussions with Yanbin Chen in the Material Science and Engineering Department at the University of Michigan. We are also grateful to Douglas Berry and Tani Kahlon, who worked on this project as undergraduate researchers.

References and Notes

(1) Rogers, J. A.; Bao, Z.; Baldwin, K.; Dodabalapur, A.; Crone, B.; Raju, V. R.; Kuck, V.; Katz, H.; Amundson, K.; Ewing, J.; Drzaic, P. *Proc. Natl. Acad. Sci.* **2001**, *98*, 4835−4840.

(2) Heringdorf, F. M.; Reuter, M. C.; Tromp, R. M. *Nature* **2001**, *412*, 517−520.

(3) Dimitrakopoulos, C. D.; Brown, A. R.; Pomp, A. *J. Appl. Phys.* **1996**, *80*, 2501−2508.

(4) Forrest, S. R. *Nature* **2004**, *428*, 911−918.

(5) Anthony, J. E.; Eaton, D. L.; Parkin, S. R. *Org. Lett.* **2002**, *4*, 15−18.

(6) Anthony, J. E.; Brooks, J. S.; Eaton, D. L.; Parkin, S. R. *J. Am. Chem. Soc.* **2001**, *123*, 9482−9483.

(7) Brooks, J. S.; Eaton, D. L.; Anthony, J. E.; Parkin, S. R.; Brill, J. W.; Sushko, Y. *Curr. Appl. Phys.* **2001**, *1*, 301−306.

(8) Haddon, R. C.; Chi, X.; Itkis, M. E.; Anthony, J. E.; Eaton, D. L.; Siegrist, Mattheus, C. C.; Palstra, T. T. M. *J. Phys. Chem. B* **2002**, *106*, 8288−8292.

(9) Sheraw, C. D.; Jackson, T. N.; Eaton, D. L.; Anthony, J. E. *Adv. Mater.* **2003**, *15*, 2009−2011.

(10) Tokumoto, T.; Brooks, J. S.; Clinite, R.; Wei, X.; Anthony, J. E.; Eaton, D. L.; Parkin, S. R. *J. Appl. Phys.* **2002**, *92*, 5208−5213.

(11) Ostroverkhova, O.; Cooke, D. G.; Shcherbyna, S.; Egerton, R. F.; Hegmann, F. A.; Tykwinski, R. R.; Anthony, J. E. *Phys. Rev. B* **2005**, *71*, 035204.

(12) Martin, D. C.; Chen, J.; Yang, J.; Drummy, L. F.; Kübel, C. *J. Polym. Sci., Part B: Polym. Phys.* **2005**, in press.

(13) Chen, J.; Anthony, J. E.; Martin, D. C. *Chem. Mater*., to be submitted for publication.

(14) Curtis, M. D.; Cao, J.; Kampf, J. W. *J. Am. Chem. Soc.* **2004**, *126*, 4318−4328.